Nordic Hydrology, 29 (4/5), 1998, 385-396
No part may be reproduced by any process without complete reference

Subpermafrost Groundwater Modelling in Ny-Ålesund, Svalbard

Paper presented at the 11th Northern Res. Basins Symposium/Workshop
Prudhoe Bay to Fairbanks, Alaska, USA – Aug. 18-22, 1997

M. Booij and A. Leijnse
Wageningen Agricultural University, The Netherlands
S. Haldorsen and M. Heim
Agricultural University of Norway
H. Rueslåtten
Statoil, Trondheim, Norway

Svalbard is a high arctic archipelago where the permafrost thickness is 150-450 m and almost continuous in ice-free areas. The model work was carried out in Ny-Ålesund, where the subpermafrost aquifers are recharged by water from the bottom of the Vestre Lovénbreen glacier. One main discharge spring is found at the entrance of an old coal mine. The computer code SUTRA has been used to simulate two-dimensional fluid movement and energy transport in the ground under steady state conditions. For the simulation, a cross section with unit thickness parallel to groundwater flow has been chosen. With the resulting output of SUTRA, contour maps of the pressure, hydraulic head, temperature and velocity have been made. Residence times for different situations have been determined to be15 years as a minimum. In general there is a good agreement between the physical reality and the simulation results.

Introduction

Subpermafrost groundwater aquifers are normally confined, with the permafrost as the confining layer. Recharge and discharge require open taliks in the permafrost. The aquifer geometry as well as the flow pattern are thus completely climatically controlled. The groundwater flow may be a major source for geothermal heat transfer and, this transfer of heat will in many places influence the distribution and thick-

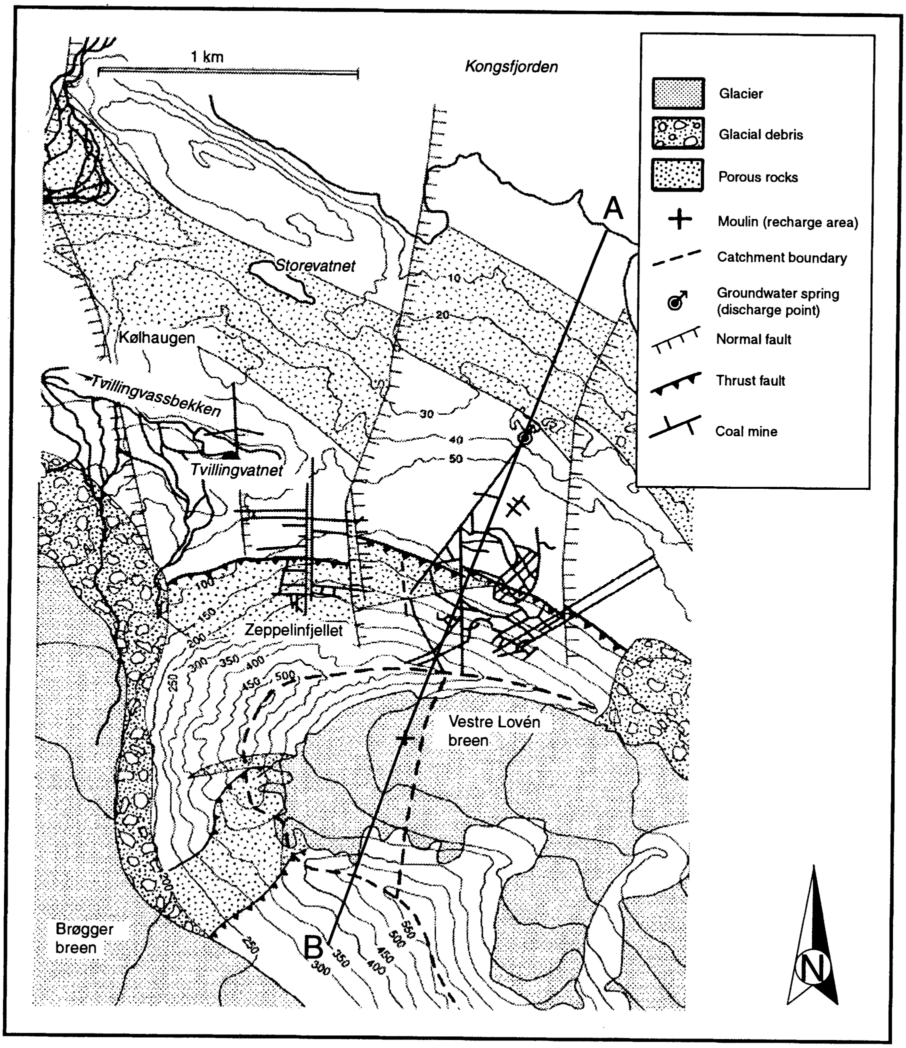

Fig. 1. Map of the Ny-Ålesund area showing glaciers, glacial debris, porous rocks, supposed groundwater catchment, groundwater spring and coal mines (modified after Orvin 1934; Haldorsen *et al.* 1996).

ness of the permafrost. It may help to maintain open discharge taliks in the permafrost also in periods when the climate becomes cooler. Climatic changes will not influence the permafrost thickness very much in a short time, but may have a fast and quite significant effect on the recharge conditions (see Haldorsen and Lauritzen 1993). Combined simulations of water flow and heat transport can form the basis for predictions of the effects of climatic changes.

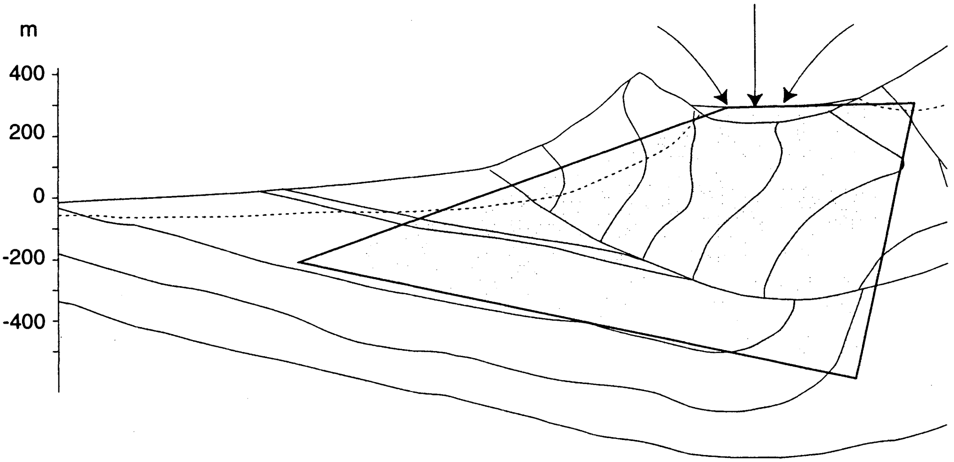

Fig. 2. Supposed lower permafrost boundary (dotted line) in cross section parallel to groundwater flow. The bedrock structures refer to the geology shown in Fig. 3. Framed area: schematised area for the simulations in Figs. 4-7. Vertical scale in metres.

This paper presents the simulations of a groundwater flow system in Ny-Ålesund, Svalbard (the Vestre Lovénbreen aquifer, Figs. 1 and 2), where quite detailed data for the underground geology and water flow are available. The underground data were collected during the coal mining periods in 1922-27 and in 1947-1963, and from around 2,000 m of bedrock cores which were drilled in 1976. The drilled cores gave us an opportunity to measure the porosity and permeabilities of the bedrock types under consideration.

Subpermafrost Groundwater Systems in Ny-Ålesund

The permafrost in Svalbard is normally rather continuous and between 150 and 450 m thick (Liestøl 1980). The recharge of groundwater occurs mainly along the temperate basal parts of the glaciers (Orvin 1944; Liestøl 1977). The groundwater flows in deep subpermafrost aquifers, and in some places it discharges in major groundwater springs, where the transfer of energy is high enough to keep the discharge channels through the permafrost open. The groundwater recharge of the Vestre Lovénbreen aquifer in Ny-Ålesund occurs in a very restricted area under the upper part of the Vestre Lovénbreen (Fig. 2) (Haldorsen and Lauritzen 1993; Haldorsen *et al.* 1996). The main discharge takes place through one of the old coal mines, where a continuous outflow of groundwater has been observed since the coal mining terminated in 1963. This seems to be the only discharge point of the aquifer (Haldorsen *et al.* 1996).

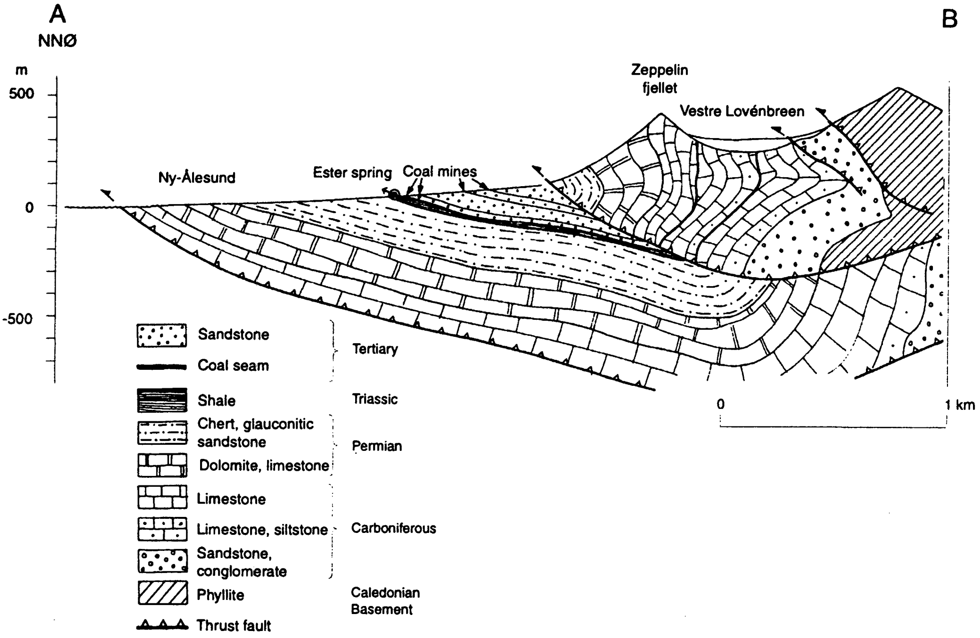

Fig. 3. Bedrock profile (A-B in Fig. 1) showing the geology along the assumed groundwater flow direction.

The Bedrock Geology and Related Hydrogeological Characteristics

The hydrogeology of the Ny-Ålesund area has been studied by Orvin (1934, 1944), Haldorsen and Lauritzen (1993) and Haldorsen *et al.* (1996), and only the major characteristics which form the basis of the modelling will be described in this paper.

Figs. 2 and 3 show the geology of the Ny-Ålesund area, and the main petrographic and hydrogeologic characteristics are listed in Table 1. The main rock types which have any significant influence upon the aquifer characteristics are from the oldest to the youngest (Challinor 1967): Carboniferous and Permian carbonate rocks (limestones and dolomites: Nordenskiöldbreen and Gipshuken Formations), Permian sandstone (Kapp Starostin Formation), Lower Triassic shale and siltstone (Vardebukt Formation) and Tertiary sandstones (Ny-Ålesund Formation).

The carbonate rocks and the Tertiary sandstones have low primary porosities and permeabilities (Table 1). The sandstone of the Kapp Starostin Formation, on the other hand, has a porosity of 0.12-0.19 and measured permeability values up to $5 \times 10^{-16} m^2$. The Kapp Starostin Formation is thus believed to make up a main bedrock aquifer, and it was also observed during the coal mining period that this rock contained significant amounts of pore water (Einar Grimsmo, pers.comm. 1992).

Table 1 – Geology of the Ny-Ålesund area with formation names used in the text, estimated thickness (Th.), rock type, porosity and permeability.

Period	Formation	Th.(m)	Rock Type	Porosity (fraction)	Permeability (m^2)
Tertiary	Ny-Ålesund	>195	sandstone, shale and coal seams	0.02-0.03 (3)	$3\cdot10^{-17}$-$6\cdot10^{-13}$ (2)
Lower Triassic	Vardebukt	0-50	shale and siltstone	0.0-0.10 (1,2)	$1\cdot10^{-20}$-$2\cdot10^{-16}$ (1,2)
Permian	Kapp Starostin	200	glauconitic sandstone and chert	0.12-0.19 (3)	$3\cdot10^{-17}$-$5\cdot10^{-11}$ (1,2)
	Gipshuken	146	dolomite	0.01-0.15 (2) $1\cdot10^{-13}$-$2\cdot10^{-9}$ (1,2)	(0.001-0.05 (2)) ($1\cdot10^{-16}$-$6\cdot10^{-13}$ (1,2))
	Nordenskiöldbreen	160	limestone and dolomite	0.01-0.15 (2) $1\cdot10^{-13}$-$2\cdot10^{-9}$ (1,2)	(0.001-0.05 (2)) ($1\cdot10^{-16}$-$6\cdot10^{-13}$ (1,2))
Carboniferous	Nordenskiöldbreen	280	limestone and dolomite	0.01-0.15 (2) $1\cdot10^{-13}$-$2\cdot10^{-9}$ (1,2)	(0.001-0.05 (2)) ($1\cdot10^{-16}$-$6\cdot10^{-13}$ (1,2))
	Brøggertind	360	sandstone and conglomerate	0.02-0.10 (3)	$3\cdot10^{-17}$-$6\cdot10^{-13}$ (2)
Precambrian	Nielsenfjellet	2500	phyllite and quartzite		

The values between brackets are estimated values for a non-karstified situation.

(1)=Brown *et al* 1977;

(2)=Domenico and Schwartz 1990;

(3)=Primary porosity and permeability measured on bedrock cores from Ny-Ålesund at Statoil's laboratorium, Trondheim.

The rocks in the Ny-Ålesund area are fractured and faulted (Fig. 1) and groundwater flows through the main fault systems. It was observed both in the 1920's and the 1960's that there often were major inflows of water into the mines when one of the main faults through the Tertiary sandstones was penetrated. We do not know to which extent the Permian and Carboniferous carbonate rocks in the fault zones and fracture zones have been dissolved and karstified and therefore form open conduits for the groundwater. This depends among other factors on the position of the rocks relative to infiltrating water, and on the amount of water which infiltrates in the rocks (van Everdingen 1981). Limestones and dolomites directly underlying those parts of the glaciers where temperatures are above the pressure-melting point (temperate zones) are reported to be karstified in other research areas in Spitsbergen (see *e.g.* Lauritzen 1991). It is therefore quite likely that the limestone which underlies the Vestre Lovénbreen is karstified as well, and that the water flows downwards through relatively wide and open channels. For this reason the permeability and porosity values in Table 1 are given for both non-karstified and karstified conditions. Both conditions are separately evaluated by the simulation model.

The Triassic Vardebukt Formation (Fig. 1 and Table 1) consists of a fine-grained shale and siltstone with low primary porosity and permeability and without open, water-conducting fractures.

Groundwater Model for the Vestre Lovénbreen Aquifer

A numerical model for groundwater flow and heat transport in the Vestre Lovénbreen aquifer has been constructed. The model is necessarily a strong simplification of the real physical system, because the available data is scarce. However, we feel confident that the main features of the groundwater system have been captured in our model.

The following simplifying assumptions have been made:

1) The groundwater system is fully saturated.
2) Both the groundwater flow and the heat transport are in steady state. This assumption is based on the observation that the recharge from the groundwater spring (Fig. 1) is almost constant in rate and temperature throughout the year (Haldorsen *et al.* 1996). As a consequence, rock and water compressibility do not play a role in the simulations.
3) The water density and viscosity are constant. This is a reasonable assumption given the small temperature differences in the system.
4) The groundwater and the solid matrix are in thermal equilibrium.
5) The groundwater flow and heat transport can be described as a two-dimensional system. Therefore, the model is based on a vertical cross section parallel to the main direction of groundwater flow.

The model domain is preferably chosen on the basis of the geological and hydrogeological data. A permafrost position as shown in Fig. 2 has been assumed. The permafrost layer has not been incorporated in the model. Instead, the lower boundary of the permafrost is used as the (left side) boundary of the groundwater model. The lower boundary of the model is formed by the Carboniferous limestone which, based on the values in Table 1, is assumed to be impermeable. The upper boundary of the model is formed by the ground surface underneath the glacier. Finally, the right side boundary has been chosen rather arbitrarily such, that its influence on the simulation results will be small.

The groundwater flow in the Vestre Lovénbreen system is a combination of fracture flow and intergranular flow. The model allows fracture flow to occur in all formations with the exception of the Triassic shale layer and the Permian sandstone. The Triassic shale layer (the Vardebukt Formation) is assumed to be an aquitard with a very low hydraulic conductivity. Groundwater flow in the Permian sandstone (the Kapp Starostin Formation) is believed mainly to be an intergranular flow. This assumption is based on observations in the 1960's, when the main leakage from the Kapp Starostin Formation seemed to be from the pore system (E. Grimsmo, pers.comm. 1992). However, this is a simplification which is only based on those historical observations, and it is not verified by recent field data.

Hydraulic parameters of the different formations have been defined accordingly (Table 1).

Recharge and Discharge

Recharge of the groundwater system takes place over a small part (25 m) of the upper boundary by meltwater and rain water flowing to the base of the glacier. The two-dimensional vertical model describes the flow through a layer with unit thickness, assuming no variations in the third co-ordinate direction. The recharge is therefore given by the total discharge (=measured discharge values for the groundwater spring: 11.7 kg/s, Haldorsen *et al.* 1996) divided by the total layer thickness over which the recharge takes place (estimated at 1,000 m). This recharge will result in an average description of the groundwater flow. In reality, however, a fully three-dimensional flow regime will exist around the recharge area, and some water particles will travel with a much higher velocity. To get an idea of the magnitude of this effect, also a situation with a five times higher recharge rate has been simulated. These two situations will be referred to as low and high recharge situations later in the paper.

Groundwater discharges from the Permian sandstone layer just below the aquitard which is made up by the Triassic shale layer. Water and heat transport to the surface through an old mine channel has not been included in the model.

Physical Parameters

The hydraulic properties of the different formations (porosity ϕ and permeability k)

Table 2 – Fluid and solid matrix properties and acceleration due to gravity with appropriate symbols, units and input values for SUTRA (based on field data and data from Weast 1968).

Fluid and solid matrix properties	Symbols	Unit	Value
Fluid compressibility	β	$m \cdot s^{-2} \cdot kg^{-1}$	0.0
Fluid specific heat	c_w	$J \cdot kg^{-1} \cdot {}^{o}C^{-1}$	4182.0
Fluid thermal diffusivity	σ_w	$J \cdot m^{-1} \cdot {}^{o}C^{-1} \cdot s^{-1}$	0.6
Density of fluid at base temperature	ρ_0	$kg \cdot m^{-3}$	1000.0
Solid matrix compressibility	α	$m \cdot s^{-2} \cdot kg^{-1}$	0.0
Solid grain specific heat	c_s	$J \cdot kg^{-1} \cdot {}^{o}C^{-1}$	849.0
Solid grain thermal diffusivity	σ_s	$J \cdot m^{-1} \cdot {}^{o}C^{-1} \cdot s^{-1}$	2.8
Density of a solid grain	ρ_s	$kg \cdot m^{-3}$	2650.0

have been defined on the basis of available data (Table 1). All geological formations are assumed to be anisotropic, with the vertical permeability one order of magnitude smaller than the horizontal permeability. Fracture flow is simulated by increasing the permeability of the formation in which such flow is assumed to take place.

The values for several fluid and solid matrix properties that govern the water and heat flow, are summarised in Table 2. The water specific heat c_w, thermal diffusivity of water σ_w and liquid density ρ_0 are given by standard values (Weast 1968). The solid matrix properties like specific heat c_s, thermal diffusivity σ_s and density ρ_s are estimated values, since no data on these physical parameters are available. No internal heat or fluid sources/sinks exist in the model domain.

The longitudinal and transversel hydrodynamic dispersivities, α_L and α_T respectively, have arbitrarily been chosen as 25 m and 2.5 m. No information on these parameters is available.

Boundary Conditions

The left side boundary of the domain is formed by the lower boundary of the permafrost zone. Since the permafrost zone is assumed to be impermeable, a no-flow boundary is defined here for the groundwater flow, while a prescribed temperature of $0^{o}C$ has been used for the heat transport. A small part of this boundary is used for the discharge of the groundwater at a prescribed pressure. The temperature of the outflowing water is calculated assuming that no heat flow due to conduction takes place across the boundary.

The largest part of the top boundary is a no-flow boundary, with the exception of that part where the rain water and meltwater of the glacier infiltrates. On that part, the mass of water entering the groundwater system is prescribed. The temperature on the top boundary and the temperature of the inflowing water are both $0^{o}C$.

The bottom boundary of the model is a no-flow boundary with a prescribed temperature. The temperature is obtained from the prevailing geothermal gradient in the region (Vågsnes and Amundsen 1993). The right side boundary is defined as a no-flow boundary for both the groundwater flow and the heat transport.

Numerical Solution

A numerical solution for the equations describing the groundwater flow and heat transport in the Vestre Lovénbreen aquifer has been obtained with the aid of the numerical code SUTRA (Voss 1984). SUTRA is a two-dimensional finite element code for coupled flow and transport of one solute or heat in a mixed saturated/unsaturated system. The code is based on a standard Galerkin finite element technique with quadrilateral elements.

For the simulations, a finite element grid of 1,600 elements was used with an average element size of 25 × 25 m. This discretisation in relation to the physical parameters of the groundwater system is such, that a stable numerical solution in terms of pressures, temperatures and groundwater velocities is obtained.

Simulation Results and Discussion

The results of the different simulations are given in Figs. 4-7 for a high recharge and low permeability situation.

The simulated pressure distributions (Fig. 4) are almost hydrostatic, with steep gradients found only near the outflow point. This is caused by the overlying low-permeable Triassic shale. The hydrostatic distribution indicates a relatively even groundwater flow without remarkable obstructions which is mainly controlled by gravity. Increasing the permeability of the medium decreases the hydraulic head gradient in the system (Fig. 5), as can be expected from Darcy's law.

Velocities in the aquifer system are virtually independent of the permeabilities, because the groundwater flow is mainly determined by the recharge since almost all boundaries are no-flow boundaries. An increase in the recharge rate therefore results in an increased groundwater velocity. Groundwater velocities vary between 10 and 30 m/year for the situation with a low recharge and between 30 and 100 m/year for the situation with high recharge (Fig. 6).

Residence times from the bottom of the glacier to the spring are found to be between 15 years for the high recharge and 400 years for the low recharge. A tritium analysis of a water sample from the spring revealed no detectable tritium at all, and a residence time of more than 30 years seems likely. The simulated residence time in the karstified limestone varied between 7 and 28 years. The chemical composition of the outflowing water indicates, however, that a long storage in carbonate rocks is unlikely, and the simulated residence times seem to be overestimated and are therefore very debatable. This feature may be caused by the fact that flow through fractures is not properly incorporated in the model.

The temperature distribution in the model (Fig. 7) is mainly determined by groundwater flow and to a smaller extent by heat conduction. The influence of the

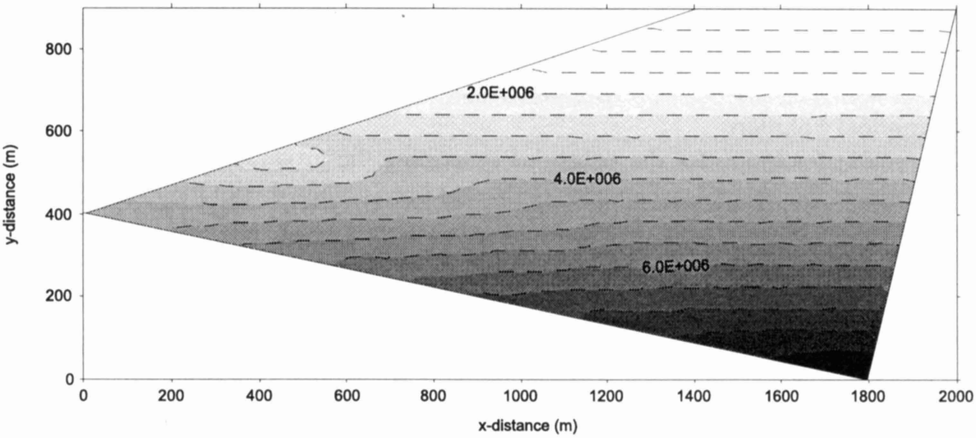

Fig. 4. Simulated pressure (Pa) for a situation with high recharge and low permeability.

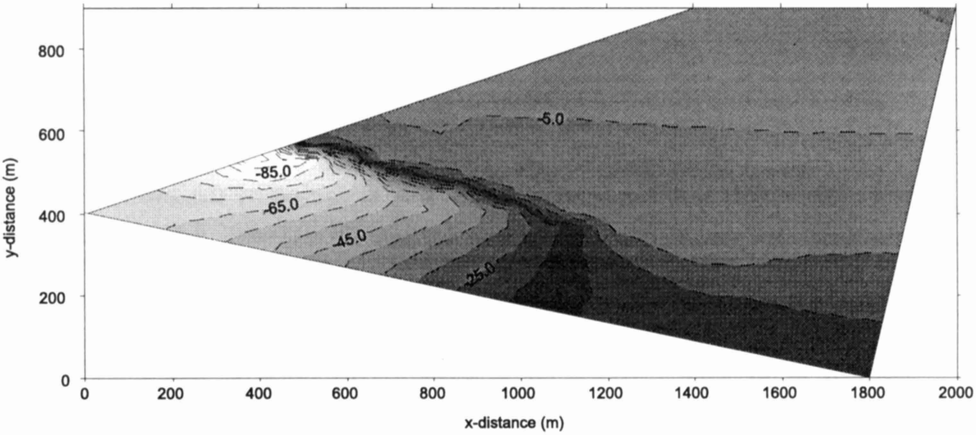

Fig. 5. Simulation of hydraulic head (m compared to the hydraulic head at inflow point) for a situation with high recharge and low permeability.

water movement is most pronounced in the simulations with high recharge. The temperature of the outflowing water in the different simulations varies between 1.7 and 4.4 °C. The measured temperature of the outflowing groundwater is 0.6°C. One should bear in mind, however, that the temperature was measured at ground surface, after the water has passed through the mine channels, and the mine channels were not incorporated in the model. Thus the simulated temperature does not contradict the measured temperature, since the water will cool down in the mine channels through the permafrost zone.

Our conclusion is that the simulation results are well in accordance with the observed field data, and it seems promising for future heat flow and water flow modelling of subpermafrost aquifers.

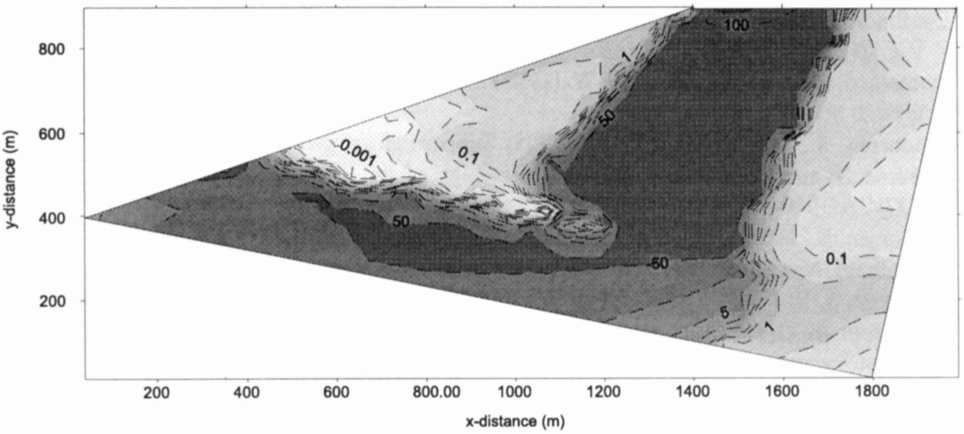

Fig. 6. Velocity (m/year) simulated for high recharge and low permeability.

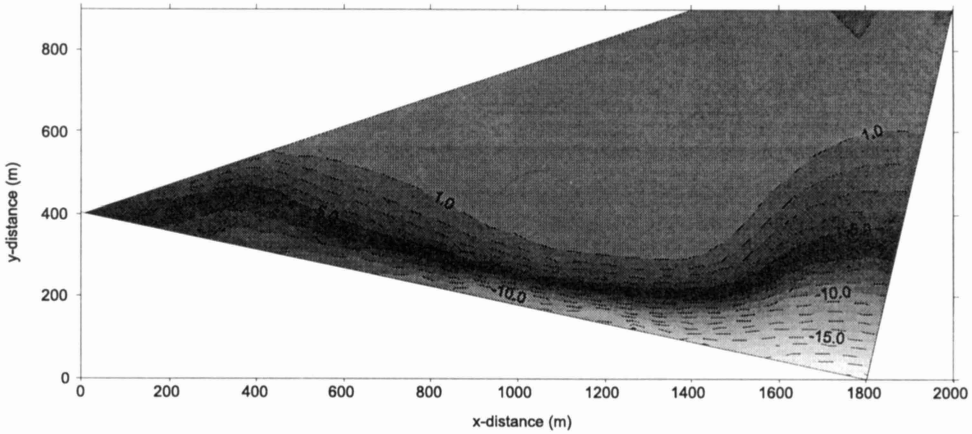

Fig. 7. Simulation of temperature (°C) for a situation with high recharge and low permeability.

Acknowledgements

Technical assistance has been provided by the Norwegian Polar Institute and Kings Bay Mining Company. Kings Bay Mining Company also placed the bedrock cores at our disposal. E. Grimsmo gave us valuable information about the water leakage into the mines during the coal mining period. L. V. Jakobsen and K. M. Haldorsen assisted in the field. Figs. 1-3 were drafted by Å. Borgan. The project was financed by grants from the Norwegian Research Council.

References

Brown, R. H., Konoplyantsev, A. A., Ineson, J., and Kovalevsky, V. S. (eds.) (1977) *Groundwater studies, an international guide for research and practice*, Unesco, Paris.

Challinor, A. (1967) The structure of Brøggerhalvøya, Spitsbergen. *Geological Magazine, Vol. 104*, pp. 322-336.

Domenico, P. A., and Schwartz, F. W. (1990) *Physical and chemical hydrogeology*, John Wiley and Sons, New York, 824 pp.

Haldorsen, S., and Lauritzen, S.-E. (1993) Subpermafrost groundwater in Spitsbergen. *In*: Banks S. and Banks. D. (eds.): Hydrogeology of hard rocks. *I.A.H. Memoires, Volume XXIV*, pp. 940-949.

Haldorsen, S., Heim, M., and Lauritzen, S.-E. (1996) Subpermafrost groundwater, Western Svalbard, *Nordic Hydrology, Vol. 27*, pp. 57-68.

Lauritzen, S.-E. (1991) Groundwater in cold climates: interaction between glacier and karst aquifers. *In*: Gjessing, Y., Hagen, J. O., Hassel, K. A., Sand, K. and Wold, B. (eds.): Arctic hydrology, present and future tasks. NHK-Report 23, pp. 139-146.

Liestøl, O. (1980) Permafrost conditions in Spitsbergen: Frost action in soils, Oslo, Publication No 21, pp. 23-28.

Liestøl, O. (1977) Pingos, springs and permafrost in Spitsbergen, *Norsk Polarinstitutts Årbok 1975*, pp. 7-29.

Orvin, A. (1934) Geology of the Kings Bay region, Spitsbergen, *Skrifter om Svalbard og Ishavet, Vol. 57*, 336 pp.

Orvin, A. (1944) Litt om kilder på Svalbard (in Norwegian), *Norsk geografisk tidsskrift, Vol. 10*, pp. 16-38.

van Everdingen, R. O. (1981) Morphology, hydrology and geochemistry of karst in permafrost terrain near Great Bear Lake, Northwest Territories, National Hydrology Research Institute, Calgary. 53 pp.

Voss, C. I. (1984) A finite element simulation model for saturated-unsaturated, fluid density dependent groundwater flow with energy transport or chemically reactive single species solute transport, USGS Water Research Invest. Rep. 84-4369, 409 pp.

Vågsnes, E., and Amundsen, H. E. F. (1993) Late Cenozoic uplift and volcanism on Spitsbergen; caused by mantle convection? *Geology, Vol. 21*, pp. 251-254.

Weast, R. C. (1988) *Handbook of chemistry and physics,* The Chemical Rubber Co., Cleveland, Ohio.

Received: November, 1997
Accepted: April, 1998

Address:
M. Booij and A. Leijnse,
Department of Water Resources,
Wageningen Agricultural University,
Nieuwe Kanaal 11 6709 PA Wageningen,
The Netherlands.
Email: +oon.leijnse@users.whh.wau.nl

H. Rueslåtten,
Statoil,
Postuttak 7004 Trondheim,
Norway.
Email: hry@statoil,no

S. Haldorsen and M. Heim,
Department of Soil and Water Sciences,
Agricultural University of Norway,
P.O.Box 5028,
N-1432 Ås,
Norway.
Email: sylvi.haldorsen@ijvf.nlh.no